A. Weiss
Department of Mechanical Engineering,
Ort Braude College of Engineering,
Karmiel, Israel
e-mail: avi@braude.ac.il

R. G. Langlois
e-mail: rlangloi@mae.carleton.ca

M. J. D. Hayes

Department of Mechanics
and Aerospace Engineering,
Carleton University Ottawa,
ON, Canada

Unified Treatment of the Kinematic Interface Between a Sphere and Omnidirectional Wheel Actuators

This paper presents a general approach to the kinematics of an orientation motion platform utilizing a sphere actuated by omnidirectional wheels. The number and type of the omnidirectional wheels, as well as their position and orientation relative to the sphere are arbitrary, provided they are distinct. In this paper, the general kinematics are presented and illustrated by sample configurations with a range of omnidirectional wheel types and quantities. Moreover, no-slip conditions are identified, and the resulting expressions and their implications on the design of such a mechanical system are demonstrated by means of several benchmark examples. [DOI: 10.1115/1.4004888]

Keywords: kinematics, parallel manipulator, omnidirectional wheels

1 Introduction

The kinematics of an ideal parallel motion platform may be argued to be such that the platform allows for an unbounded range of motion, both angular and translational, while having a singularity-free, fully dexterous workspace and complete decoupling of the translational degrees of freedom (DOF) from the rotational ones. Many parallel platform architectures exist, the most well known of which are the Gough Platform [1] and the similar Stewart Platform [2], which are widely used. This style of motion platform, based on six extendable legs connected in parallel, can carry much heavier payloads than similarly scaled serial counterparts. However, they have relatively small ranges of motion, singularities within the reachable workspace, while the translational and rotational DOF are tightly coupled, leading to complex mathematical formulations for platform kinematics, dynamics, and control. Significant research on determining the workspace of these platforms exists, see, for example, Gosselin [3]. Some attempts have been made to resolve some of the aforementioned issues. Yan et al. [4] suggest a platform that decouples the translational degrees of freedom from the rotational ones. However, singularities within the workspace, limited payload capacity, as well as a limited range of angular motion result. Unbounded rotational motion is achieved by the Eclipse II architecture [5]; however, it is not singularity-free and the kinematics are very complicated and require numerical solutions. Advani [6] shows ways to optimize the kinematic design of parallel platforms based on prescribed characteristics, but the methods are exclusive to six-legged Stewart-style platforms. Kinematic design optimization is the concern of many research publications, such as Stock et al. [7], Fattah et al. [8] for cable suspended platforms, and Merlet [9], to name a few. Merlet [10], in his book on the subject, gives thorough analysis and synthesis approaches for various parallel platforms, including spherical platforms. Still, the issues mentioned above remain. The Atlas platform [11] achieves singularity-free unbounded rotational motion utilizing three omnidirectional wheels driving a sphere (Fig. 1). Utilizing friction wheels to drive a sphere is presented also by Lauwers et al. [12] with simple friction wheels, and by Ferrier and Raucent [13], where a sphere is actuated for a single DOF by means of a single omnidirectional wheel. The work of West et al. [14] shows how to use a ball wheel for a single degree of freedom actuation with the remaining degrees of freedom passive such that there is no slip. Three such ball wheels may be utilized similarly to omnidirectional wheels with rollers on their periphery to drive a wheeled mobile robot on a plane. Similarly, Williams et al. [15], and Saha et al. [16] utilize three omnidirectional wheels to drive a mobile robot or vehicle on a plane. Most of the research involving omnidirectional wheels concentrates on wheeled mobile robots, where an extensive amount of literature already exists for the kinematics of mobile robots with standard wheels (see Alexander et al. [17], Low et al. [18] to name a few), and offset castor wheels (see Yu et al. [19]).

In the Atlas architecture, orienting is decoupled from positioning, and unbounded rotation is possible about any axis. The decoupling is accomplished by fixing a three degree of freedom spherical orienting platform on a linear platform with three orthogonal translational directions. The key to the design is the use of three omnidirectional wheels which impart angular displacements to the sphere, thereby providing rotational actuation. The kinematics for the Atlas platform have been developed in Refs. [20 and 21] and yield a simple expression for an ideal case. These promising results are applied here to more detailed and thorough investigation of the concept of driving a sphere with active three degrees of freedom utilizing omnidirectional wheels, minimizing or completely eliminating slip, while taking the inherent imperfections of the various designs of omnidirectional wheels. While different types of omnidirectional wheels have been investigated previously (see Refs. [22 and 23]); this paper presents the unified kinematics of a sphere actuated by omnidirectional wheels, where the wheel type, the number of wheels, the contact point positions, and orientations are kept general. In addition, slip and no-slip conditions are identified and preferred configurations are discussed.

2 The Generalized Problem

A generalization of the Atlas platform problem is to define the orienting platform as a sphere actuated by omnidirectional wheels positioned at n arbitrary contact points and arranged in arbitrary orientations. Thus, the Atlas platform is a specific case of the generalized problem, where $n=3$. The theoretical kinematics problem then becomes finding a geometrical configuration for the omnidirectional wheels such that the slip due to kinematic issues is zero. To develop the kinematics of the platform, a general configuration is assumed, and an inertial coordinate frame is

Contributed by the Mechanisms and Robotics Committee Division of ASME for publication in the JOURNAL OF MECHANISMS AND ROBOTICS. Manuscript received June 12, 2009; final manuscript received June 29, 2011; published online September 26, 2011. Assoc. Editor: Frank C. Park.

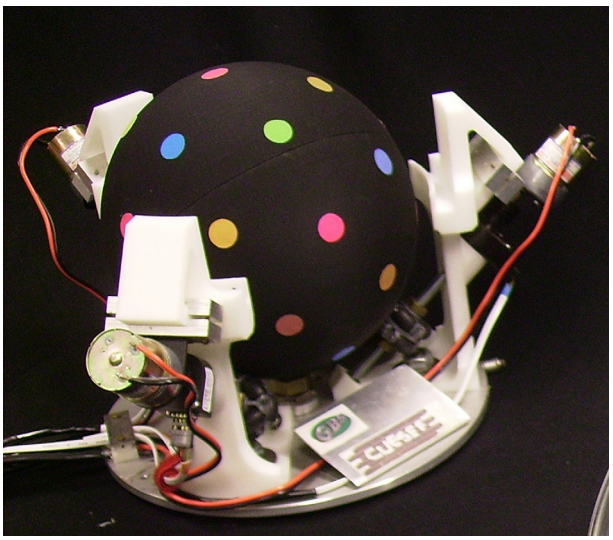

Fig. 1 The Atlas table-top demonstrator highlighting the omnidirectional wheel actuation concept

positioned at the geometric centre of the sphere as illustrated in Fig. 2. The kinematic slip is defined as the difference between the linear velocity $\vec{\mathbf{V}}_\mathbf{i}$ induced by the actuating wheel i at its contact point with the sphere and the velocity of the same contact point $\vec{\mathbf{V}}'_\mathbf{i}$ on the sphere. It must be stated here that the no-kinematic slip condition is a necessary condition for achieving zero slip in the system.

The translational motion, generated with an XYZ gantry, is completely decoupled from the rotational motion of the sphere; thus, the velocity of the geometric centre of the sphere is simply the velocity dictated by the gantry. The resulting rectilinear motion is straightforward and well understood and will not be further discussed. Since an omnidirectional wheel allows free rolling in the direction perpendicular to the actuation direction [24,25], the no-slip requirement for this direction does not apply. While a generalized approach to finding the instantaneous screw based on velocities of three points on a rigid body exists [25,26], it requires perfect knowledge of these velocities, i.e., three components of the velocity for each given point. In the problem presented here, only two components of the velocity per contact point are known, namely, the actuation direction and the zero-velocity in the radial direction of the sphere. Hence, the approach in Refs. [25 and 26] may not be utilized as presented. The omnidirectional wheels are treated as ideal, meaning that the contact point is assumed to be constant. The change in contact point due to omnidirectional wheel design, such as dual-row omnidirectional wheels is not within the scope of this paper. However, the effect of the changing contact point simply leads to a set of constant correction matrices that modify the basic Jacobian presented in this paper [22].

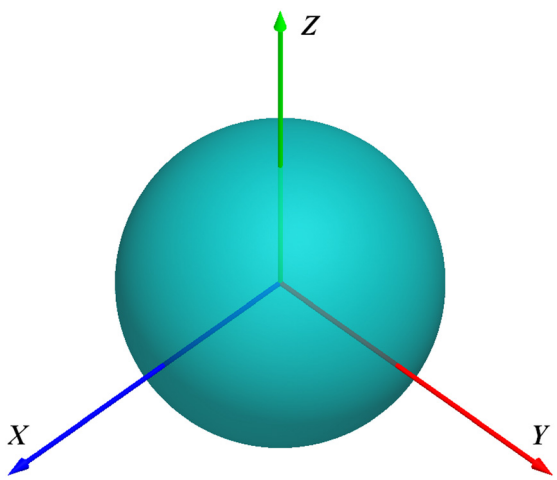

Fig. 2 Inertial coordinate frame with origin at the geometric centre of the sphere

All mathematical developments presented here are referenced to the inertial coordinate frame illustrated in Fig. 1. $\vec{\mathbf{R}}_\mathbf{i}$ are the position vectors of the contact points and $\vec{\Omega}$ is the angular velocity of the sphere. The contact point velocity on the sphere side of the sphere/omnidirectional wheel interface is therefore

$$\vec{\mathbf{V}}'_\mathbf{i} = \vec{\Omega} \times \vec{\mathbf{R}}_\mathbf{i} \tag{1}$$

where subscript i refers to a specific omnidirectional wheel. The velocity of the contact point on the omnidirectional wheel side can be broken into two components: one in the actuation direction, and the other in the direction of the free-roll of the castors

$$\vec{\mathbf{V}}_\mathbf{i} = V_i \hat{\mathbf{v}}_\mathbf{i} + V_{ri} \hat{\mathbf{v}}_\mathbf{ri} \tag{2}$$

where $\hat{\mathbf{v}}_\mathbf{i}$ is a unit vector in the actuation direction, and $\hat{\mathbf{v}}_\mathbf{ri}$ is a unit vector in the free-roll direction. These two directions are orthogonal by design, such that

$$\hat{\mathbf{v}}_\mathbf{i} \cdot \hat{\mathbf{v}}_\mathbf{ri} = 0 \tag{3}$$

The no-slip requirement may now be restated as

$$(\vec{\Omega} \times \vec{\mathbf{R}}_\mathbf{i}) \cdot \hat{\mathbf{v}}_\mathbf{i} = V_i \tag{4}$$

or, alternatively stated in words, the magnitude of the velocity of a sphere contact point with the omnidirectional wheel in the actuation direction is required to be the same as the one on the omnidirectional wheel in the same direction, thereby eliminating slip. Eq. (4) can be rearranged using vector product relations as

$$(\vec{\Omega} \times \vec{\mathbf{R}}_\mathbf{i}) \cdot \hat{\mathbf{v}}_\mathbf{i} = (\vec{\mathbf{R}}_\mathbf{i} \times \hat{\mathbf{v}}_\mathbf{i}) \cdot \vec{\Omega} = V_i \tag{5}$$

Since the magnitude of all position vectors is the radius of the sphere, R, the position vectors of the contact points can be written as

$$\vec{\mathbf{R}}_\mathbf{i} = R\hat{\mathbf{R}}_\mathbf{i} \tag{6}$$

where $\hat{\mathbf{R}}_\mathbf{i}$ is a unit vector in the direction of contact point i from the sphere centre. Eq. (5) can then be rewritten as

$$(\hat{\mathbf{R}}_\mathbf{i} \times \hat{\mathbf{v}}_\mathbf{i}) \cdot \vec{\Omega} = \frac{V_i}{R} \tag{7}$$

Now, since the actuation velocity of the omnidirectional wheel may be expressed as

$$V_i \hat{\mathbf{v}}_\mathbf{i} = \vec{\omega}_\mathbf{i} \times \vec{\mathbf{r}}_\mathbf{i} \tag{8}$$

where ω_i is the magnitude of the angular velocity of omnidirectional wheel i and r_i is its radius, the contact point actuation velocity can be expressed as

$$V_i = \omega_i r_i \tag{9}$$

Thus

$$(\hat{\mathbf{R}}_\mathbf{i} \times \hat{\mathbf{v}}_\mathbf{i}) \cdot \vec{\Omega} = \frac{r_i}{R}\omega_i \tag{10}$$

defining the unit induced angular velocities, $\hat{\Omega}_i$ as

$$\hat{\Omega}_i = \hat{\mathbf{R}}_\mathbf{i} \times \hat{\mathbf{v}}_\mathbf{i} \tag{11}$$

yields

$$\hat{\Omega}_i \cdot \vec{\Omega} = \frac{r_i}{R}\omega_i \tag{12}$$

Equation (12) defines a relationship between $\vec{\Omega}$, the angular velocity of the sphere, and ω_i, the actuation angular velocities of the omnidirectional wheels, which defines the kinematics of the system. Thus, for n contact points, we obtain the following matrix equation in component form

$$\begin{bmatrix} \hat{\Omega}_1^T \\ \hat{\Omega}_2^T \\ \hat{\Omega}_3^T \\ . \\ . \\ \hat{\Omega}_n^T \end{bmatrix} \vec{\Omega} = \frac{1}{R} \begin{bmatrix} r_1 & 0 & . & . & . & \\ 0 & r_2 & 0 & . & . & . \\ 0 & 0 & r_3 & . & . & . \\ . & . & . & . & . & . \\ . & . & . & . & . & . \\ . & . & . & . & . & r_n \end{bmatrix} \begin{Bmatrix} \omega_1 \\ \omega_2 \\ \omega_3 \\ . \\ . \\ \omega n \end{Bmatrix} \tag{13}$$

The relationship in Eq. (13) is valid as long as there is a solution to this system of n equations. There are three cases to consider here, $n<3$, $n=3$, and $n>3$.

2.1 The $n<3$ Case. In the case where $n<3$, there are more degrees of freedom than equations; thus, while slip-free conditions exist, singularities also exist due to the extra degrees of freedom. This case is not suitable for a three DOF orientation platform, and is not further discussed.

2.2 The $n=3$ Case. In this case, the system of equations reduces to

$$\begin{bmatrix} \hat{\Omega}_1^T \\ \hat{\Omega}_2^T \\ \hat{\Omega}_3^T \end{bmatrix} \vec{\Omega} = \frac{1}{R} \begin{bmatrix} r_1 & 0 & 0 \\ 0 & r_2 & 0 \\ 0 & 0 & r_3 \end{bmatrix} \begin{Bmatrix} \omega_1 \\ \omega_2 \\ \omega_3 \end{Bmatrix} \tag{14}$$

and, in this case, the requirement for no-slip is that the matrix

$$\begin{bmatrix} \hat{\Omega}_1^T \\ \hat{\Omega}_2^T \\ \hat{\Omega}_3^T \end{bmatrix} \tag{15}$$

be nonsingular. To satisfy this, it is required that the three unit vectors $\hat{\Omega}_i$ be linearly independent. In this case, the system will have zero slip, and the kinematics of the system are given by

$$\vec{\Omega} = \frac{1}{R} \begin{bmatrix} \hat{\Omega}_1^T \\ \hat{\Omega}_2^T \\ \hat{\Omega}_3^T \end{bmatrix}^{-1} \begin{bmatrix} r_1 & 0 & 0 \\ 0 & r_2 & 0 \\ 0 & 0 & r_3 \end{bmatrix} \begin{Bmatrix} \omega_1 \\ \omega_2 \\ \omega_3 \end{Bmatrix} \tag{16}$$

or in Jacobian form

$$\vec{\Omega} = \mathbf{J}\vec{\omega} \tag{17}$$

where

$$\vec{\omega} = \{ \omega_1 \quad \omega_2 \quad \omega_3 \}^T \tag{18}$$

and

$$\mathbf{J} = \frac{1}{R} \begin{bmatrix} \hat{\Omega}_1^T \\ \hat{\Omega}_2^T \\ \hat{\Omega}_3^T \end{bmatrix}^{-1} \begin{bmatrix} r_1 & 0 & 0 \\ 0 & r_2 & 0 \\ 0 & 0 & r_3 \end{bmatrix} \tag{19}$$

Since the Jacobian of the system is constant once the configuration has been determined, acceleration-level kinematics can be derived by differentiation of Eq. (19) yielding

$$\dot{\vec{\Omega}} = \mathbf{J}\dot{\vec{\omega}} \tag{20}$$

Obtaining the expression for the orientation of the platform, however, is not as simple. To accomplish that, quaternions or Euler parameters are the natural choice since the unbounded and singularity-free nature of the design calls for a singularity-free representation. Thus, integration of the quaternionic differential equation [27]

$$\dot{q} = \frac{1}{2}\Omega \circ q \tag{21}$$

is required, where q is the unit quaternion describing the orientation of the system, and $\Omega \circ q$ is a quaternionic product. Finally, the inverse kinematics of the system relating the required omnidirectional wheel speeds to the desired sphere angular velocity is

$$\mathbf{J}^{-1} = R \begin{bmatrix} \frac{1}{r_1} & 0 & 0 \\ 0 & \frac{1}{r_2} & 0 \\ 0 & 0 & \frac{1}{r_3} \end{bmatrix} \begin{bmatrix} \hat{\Omega}_1^T \\ \hat{\Omega}_2^T \\ \hat{\Omega}_3^T \end{bmatrix} \tag{22}$$

2.3 The $n>3$ Case. The motivation for performing the analysis for the $n>3$ case is twofold. First, generalizing the problem to seek other potential solutions may allow for improved designs. Second, the triple-race omnidirectional wheels may have either one or two contact points per wheel and having three of these imply having more than three contact points with the sphere. Generalizing the problem to n contact points serves as the analysis tool for the kinematics of such systems. In the case where $n>3$, we have an overdetermined set of equations. This case usually calls for approximation, typically using a least squares approach. However, the actual kinematics will be determined by the dynamics of the system in this case, and the least square approximation would yield the best case scenario and would help determine the case with minimum overall slip, thus minimal energy loss in the motion transfer system and implicitly the most direct relationship between control inputs and platform motion.

Rewriting Eq. (13) in matrix notation, we have

$$[\Omega^T]\vec{\Omega} = \frac{1}{R}[r]\vec{\omega} \tag{23}$$

where

$$[\Omega^T] = \begin{bmatrix} \hat{\Omega}_1^T \\ \hat{\Omega}_2^T \\ \hat{\Omega}_3^T \\ . \\ . \\ \hat{\Omega}_n^T \end{bmatrix} \tag{24}$$

While the forward kinematics of the system is an overdetermined set of equations, the inverse kinematics is straightforward. Knowing the desired angular velocity vector we can easily calculate the input angular velocities required to obtain the desired output. Thus

$$\vec{\omega} = R[r]^{-1}[\Omega^T]\vec{\Omega} \tag{25}$$

The forward kinematics, however, requires approximation. The solution to the forward kinematics in the least square sense, yields

$$\vec{\Omega}_{ls} \approx \frac{1}{R}\{[\Omega][\Omega^T]\}^{-1}[\Omega][r]\,\vec{\omega} \tag{26}$$

where

$$[\Omega] = \left[\Omega^T\right]^{\mathrm{T}} \tag{27}$$

which can be approximated as

$$\vec{\Omega}_{ls} \approx \mathbf{J_{ls}}\vec{\omega} \tag{28}$$

and the Jacobian for the least squares approximation is

$$\mathbf{J_{ls}} = \frac{1}{R}[\Omega_3]^{-1}[\Omega][r] \tag{29}$$

To evaluate the slip at the contact points, it is necessary to compare the contact point velocity on the sphere to the contact point velocity on the omnidirectional wheel.

It was shown earlier that the contact point velocity on the omnidirectional wheel is:

$$\vec{\mathbf{V}}_{\mathbf{o_i}} = \omega_i r_i \hat{v}_i \tag{30}$$

and the contact point velocity on the sphere side is

$$\vec{\mathbf{V}}_{\mathbf{s_i}} = \vec{\Omega}_{ls} \times \vec{\mathbf{R}}_{\mathbf{i}} \tag{31}$$

Thus, the velocity difference in the actuating direction is

$$\Delta V_i = \|\vec{\mathbf{V}}_{\mathbf{o_i}}\| - \vec{\mathbf{V}}_{\mathbf{s_i}} \cdot \hat{v}_i \tag{32}$$

The slip ratio can be defined as

$$S_i \equiv \frac{\Delta V_i}{\|\vec{\mathbf{V}}_{\mathbf{o_i}}\|} = 1 - \frac{\vec{\mathbf{V}}_{\mathbf{s_i}} \cdot \hat{v}_i}{\|\vec{\mathbf{V}}_{\mathbf{o_i}}\|} \tag{33}$$

and an overall slip assessment indicator would be

$$S = \sqrt{\sum_{i=1}^{n} S_i^2} \tag{34}$$

where the minimal value for S is desired.

While in the general case, it is clear that having more than three omnidirectional wheels driving the sphere leads to slip and energy loss, a larger number of omnidirectional wheels may be utilized without slip if the velocities of the redundant omnidirectional wheels are coordinated such that their slip factors will all be zero, resulting in a master-slave system, where three omnidirectional wheels determine the angular velocity of the sphere and the remaining match their speeds such that slip is zero. To obtain that, three omnidirectional wheels need to be selected such that they meet the criteria set out for the $n = 3$ case, such that the resulting sphere angular velocity is evaluated, then the required velocities at the remaining contact points are obtained resulting in zero slip. Although there is no kinematic benefit from such a master-slave system, benefits that stem from dynamics, vibration, and stress considerations can exist. Since omnidirectional wheels must have some gaps between their rollers, there are areas where loss of contact may occur, thus having a second omnidirectional wheel covering the same degree of freedom allows compensating for this problem as detailed below.

3 Omnidirectional Wheel Types and Their Effect on the Kinematics

In the preceding discussion, the omnidirectional wheels were assumed to be perfectly round, while in reality, it is impossible to have a perfectly round omnidirectional wheel as illustrated in (Fig. 3). A simple solution to the discontinuity problem caused by the basic design of omnidirectional wheels is utilizing a dual-race omnidirectional wheel (Fig. 4).

This addresses the problem of obtaining continuous contact with the sphere; however, it introduces a shift in the location of the contact points on the sphere, thereby introducing complications in the kinematics of the system that are shown to produce significant errors both in magnitude (4%) and in direction of the angular velocity vector of the sphere (3 deg) as detailed in Ref. [22], and thus possibly control issues.

This problem could be avoided by splitting the dual-row omnidirectional wheels, having the two rows mounted on separate races that touch on antipodal points on the sphere. Antipodal points on the sphere would have the same velocity in the actuation direction. For a contact point $\vec{\mathbf{R}}_{\mathbf{1}}$ with actuation direction $\hat{v}_1$, we have the velocity $\vec{\mathbf{V}}_{\mathbf{1}} = \vec{\Omega} \times \vec{\mathbf{R}}_{\mathbf{1}}$. It is clear that for the point located on the same great circle but angularly offset by 180 deg, we have $\vec{\mathbf{R}}_{\mathbf{2}} = -\vec{\mathbf{R}}_{\mathbf{1}}$ and the velocity $\vec{\mathbf{V}}_{\mathbf{2}} = \vec{\Omega} \times \vec{\mathbf{R}}_{\mathbf{2}} = -\vec{\Omega} \times \vec{\mathbf{R}}_{\mathbf{1}} = -\vec{\mathbf{V}}_{\mathbf{1}}$ that is, the same magnitude but opposite in direction. Thus, setting the actuation direction to be $\hat{v}_2 = -\hat{v}_1$, we obtain an equivalent second row at $\vec{\mathbf{R}}_{\mathbf{2}}$ enslaved to the omnidirectional wheel at $\vec{\mathbf{R}}_{\mathbf{1}}$. All that is left is to arrange the omnidirectional wheels such that the rollers are synchronized between the two races, a relatively easy task since

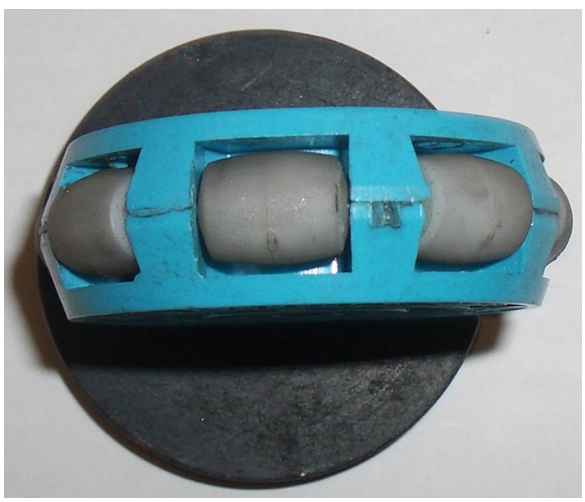

Fig. 3 A single-race omnidirectional wheel

Fig. 4 A dual-race omnidirectional wheel

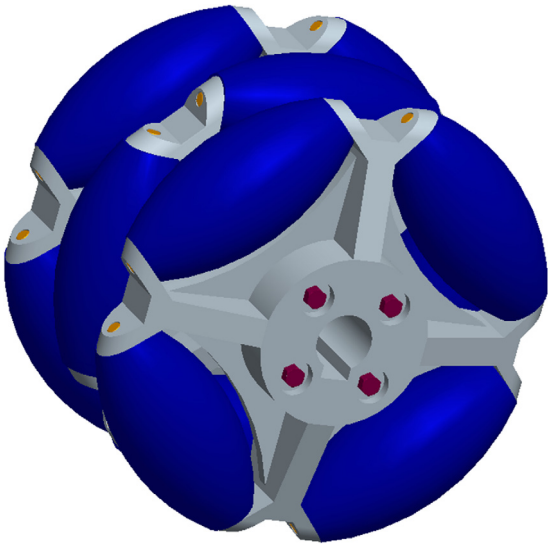

Fig. 5 A triple-race omnidirectional wheel

the actuation speeds for both wheels are identical and they could, in principle, be actuated by the same motor.

Another attempt to combine the benefits of the single and dual-row designs, driven by intuition, is to have triple-race omnidirectional wheels (Fig. 5), such that the two external races touch the sphere at the same time, alternating with the centre race, yielding an equivalent or effective contact point that is exactly in between them, and thus generating continuous contact with a continuous effective contact point.

Utilizing three dual-race omnidirectional wheels instead of single-race ones, changes the kinematics due to the shift of contact points when shifting between the two races of each omnidirectional wheel occurs, as presented in Ref. [22]. However, the problem remains one with $n=3$, since at any instance, there are exactly three contact points.

Utilizing three triple-race omnidirectional wheels, however, is a completely different case. Triple-race omnidirectional wheels, alternate between one point of contact when the centre race is in contact with the sphere, and two points of contact when the two outer races are in contact with the sphere simultaneously. This in turn, creating a variety of combinations, where anywhere between three and six contact points (i.e., $n=3,4,5,6$) could exist, and where all combinations will be encountered during typical operation. However, this case has simplifying constraints, since any two simultaneous contact points belonging to a single omnidirectional wheel, share the same r, ω, and $\hat{v}$. This allows for the simplification of the equations. In the worst case scenario, where $n=6$, the kinematics are given by

$$\begin{bmatrix} \hat{\Omega}_{11}^T \\ \hat{\Omega}_{12}^T \\ \hat{\Omega}_{21}^T \\ \hat{\Omega}_{22}^T \\ \hat{\Omega}_{31}^T \\ \hat{\Omega}_{32}^T \end{bmatrix} \vec{\Omega} = \frac{1}{R} \begin{bmatrix} r_1 & 0 & 0 & 0 & 0 & 0 \\ 0 & r_1 & 0 & 0 & 0 & 0 \\ 0 & 0 & r_2 & 0 & 0 & 0 \\ 0 & 0 & 0 & r_2 & 0 & 0 \\ 0 & 0 & 0 & 0 & r_3 & 0 \\ 0 & 0 & 0 & 0 & 0 & r_3 \end{bmatrix} \begin{Bmatrix} \omega_1 \\ \omega_1 \\ \omega_2 \\ \omega_2 \\ \omega_3 \\ \omega_3 \end{Bmatrix} \tag{35}$$

where

$$\hat{\Omega}_{ij} = \hat{R}_{ij} \times \hat{v}_i \tag{36}$$

and $\hat{R}_{ij}$ is a unit vector in the direction of the contact point j of omnidirectional wheel i.

As presented above, this kind of over-determined equation set is usually solved utilizing an approximation method similar to least squares. However, using such an approach leads to a solution that is missing the point of the design: to achieve motion that is equivalent to that induced by the contact point of the centre race. It should be expected that any set of two equations belonging to the same omnidirectional wheel will yield a result in the same direction as the equivalent result for the single-race case. While this may be accomplished by utilizing the results from the single-race analysis, the equations are still over constrained. Solutions can only be approximated, which implies that the slip-free condition may not be satisfied. Thus, without being able to achieve slip-free conditions, the kinetics of the system must be taken into consideration, and the true motion cannot be determined using kinematics alone.

Rearranging the terms in Eq. (35), yields another way to look at the problem

$$\begin{bmatrix} \hat{\Omega}_{11}^T & -\frac{r_1}{R} & 0 & 0 \\ \hat{\Omega}_{12}^T & -\frac{r_1}{R} & 0 & 0 \\ \hat{\Omega}_{21}^T & 0 & -\frac{r_2}{R} & 0 \\ \hat{\Omega}_{22}^T & 0 & -\frac{r_2}{R} & 0 \\ \hat{\Omega}_{31}^T & 0 & 0 & -\frac{r_3}{R} \\ \hat{\Omega}_{32}^T & 0 & 0 & -\frac{r_3}{R} \end{bmatrix} \begin{Bmatrix} \Omega_x \\ \Omega_y \\ \Omega_z \\ \omega_1 \\ \omega_2 \\ \omega_3 \end{Bmatrix} = \vec{0} \tag{37}$$

This representation allows once again examining a given design. In order to obtain a nontrivial solution, it is required for the determinant of the matrix in Eq. (37) to be zero. Once this is established, there could be sets of allowable solutions $\{\vec{\Omega}, \vec{\omega}\}$ that yield slip-free conditions.

Gaussian elimination further simplifies the equations, yielding

$$\begin{bmatrix} \hat{\Omega}_{11}^T & -\frac{r_1}{R} & 0 & 0 \\ \hat{\Omega}_{12}^T - \hat{\Omega}_{11}^T & 0 & 0 & 0 \\ \hat{\Omega}_{21}^T & 0 & -\frac{r_2}{R} & 0 \\ \hat{\Omega}_{22}^T - \hat{\Omega}_{21}^T & 0 & 0 & 0 \\ \hat{\Omega}_{31}^T & 0 & 0 & -\frac{r_3}{R} \\ \hat{\Omega}_{32}^T - \hat{\Omega}_{31}^T & 0 & 0 & 0 \end{bmatrix} \begin{Bmatrix} \Omega_x \\ \Omega_y \\ \Omega_z \\ \omega_1 \\ \omega_2 \\ \omega_3 \end{Bmatrix} = \vec{0} \tag{38}$$

Rows 1, 3, and 5 of the coefficient matrix of Eq. (38) are clearly linearly independent with respect to each other, and with respect to rows 2, 4, and 6. All that remains is to ensure that the determinant of the smaller (3×3) matrix

$$\begin{bmatrix} \hat{\Omega}_{12}^T - \hat{\Omega}_{11}^T \\ \hat{\Omega}_{22}^T - \hat{\Omega}_{21}^T \\ \hat{\Omega}_{32}^T - \hat{\Omega}_{31}^T \end{bmatrix} \tag{39}$$

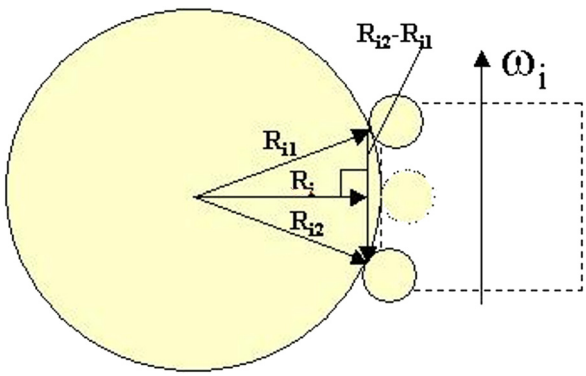

Fig. 6 Contact point geometry when two races touch the sphere simultaneously

is zero. Remembering that $\hat{\Omega}_{ij} = \hat{R}_{ij} \times \hat{v}_i$, the rows of the matrix in Eq. (39) may be rewritten as

$$\hat{\Omega}_{i2} - \hat{\Omega}_{i1} = (\hat{R}_{i2} - \hat{R}_{i1}) \times \hat{v}_i \tag{40}$$

From the geometry of the problem, illustrated in Fig. 6, it is concluded that the result is a vector in the direction of $\hat{R}_i$. Hence, the matrix above can be rewritten as

$$\begin{bmatrix} \hat{R}_1^T \\ \hat{R}_2^T \\ \hat{R}_3^T \end{bmatrix} \tag{41}$$

The no-slip condition now becomes a requirement on the position vectors of the effective contact points to be linearly dependent. Finally, combining this requirement with the no-slip requirement on the centre row combination, which was shown to be that the matrix

$$\begin{bmatrix} \hat{\Omega}_1^T \\ \hat{\Omega}_2^T \\ \hat{\Omega}_3^T \end{bmatrix} \tag{42}$$

be nonsingular; denotes the need for $\hat{R}_i$ to be linearly dependent while $\hat{\Omega}_i$ are linearly independent.

4 Examples

4.1 The Orthogonal Case. The following example examines an architecture, illustrated in Fig. 7, that satisfies the necessary condition developed above, and indeed yields zero kinematic slip. While this architecture is fairly simple, it provides a good benchmark to demonstrate the principles and point out the problems without the need for cumbersome expressions. For simplicity, and without loss of generality, the global coordinate frame is the one in Fig. 7. This allows all calculations to be performed directly in the global coordinate frame.

The sphere has radius R, and each of the omnidirectional wheels has radius r. Thus, the position vectors of the three contact points are

$$\vec{\mathbf{R}}_1 = R\hat{\mathbf{i}}; \quad \vec{\mathbf{R}}_2 = R\hat{\mathbf{j}}; \quad \vec{\mathbf{R}}_3 = R\hat{\mathbf{k}} \tag{43}$$

and the position vectors of the contact points with respect to the omnidirectional wheel centres of rotation are

$$\vec{\mathbf{r}}_1 = -r\hat{\mathbf{i}}; \quad \vec{\mathbf{r}}_2 = -r\hat{\mathbf{j}}; \quad \vec{\mathbf{r}}_3 = -r\hat{\mathbf{k}} \tag{44}$$

The angular velocities of the omnidirectional wheels are

$$\vec{\omega}_1 = \omega_1\hat{\mathbf{j}}; \quad \vec{\omega}_2 = \omega_2\hat{\mathbf{k}}; \quad \vec{\omega}_3 = \omega_3\hat{\mathbf{i}} \tag{45}$$

and therefore, the velocities they induce on the sphere at the contact points are,

$$\begin{aligned} \vec{\mathbf{V}}_1 &= \vec{\omega}_1 \times \vec{\mathbf{r}}_1 = \omega_1 r\hat{\mathbf{k}} \\ \vec{\mathbf{V}}_2 &= \vec{\omega}_2 \times \vec{\mathbf{r}}_2 = \omega_2 r\hat{\mathbf{i}} \\ \vec{\mathbf{V}}_3 &= \vec{\omega}_3 \times \vec{\mathbf{r}}_3 = \omega_3 r\hat{\mathbf{j}} \end{aligned} \tag{46}$$

respectively. These velocities create the three components of angular velocity of the sphere

$$\hat{\Omega}_1 = \hat{\mathbf{i}} \times \hat{\mathbf{k}} = -\hat{\mathbf{j}}; \qquad \hat{\Omega}_2 = \hat{\mathbf{j}} \times \hat{\mathbf{i}} = -\hat{\mathbf{k}}; \qquad \hat{\Omega}_3 = \hat{\mathbf{k}} \times \hat{\mathbf{j}} = -\hat{\mathbf{i}} \tag{47}$$

It is clear now that these are mutually orthogonal, since

$$\hat{\Omega}_i \cdot \hat{\Omega}_j = 0 \ldots i \neq j \tag{48}$$

This could alternatively be shown directly by evaluating the Jacobian of the system as

$$\mathbf{J} = \frac{r}{R}\begin{bmatrix} 0 & -1 & 0 \\ 0 & 0 & -1 \\ -1 & 0 & 0 \end{bmatrix}^{-1} = \frac{r}{R}\begin{bmatrix} 0 & 0 & -1 \\ -1 & 0 & 0 \\ 0 & -1 & 0 \end{bmatrix} \tag{49}$$

noting that the rows are linearly independent as required for the single-row case. It is obvious, however, that this case does not simultaneously fulfill the requirement for $n = 6$.

4.2 The Atlas Sphere. The current configuration of the Atlas motion platform [28] has the three omnidirectional wheels arranged on the edges of an equilateral triangle with an elevation angle of 40 deg. The reason for the equilateral configuration is to achieve as even force and torque distribution on the omnidirectional wheels as possible; however, the elevation angle of 40 deg was chosen for the demonstrator solely due to ease of manufacturing and assembly. To generalize the equilateral configuration, an arbitrary elevation angle θ will be used. The configuration is presented in Fig. 8.

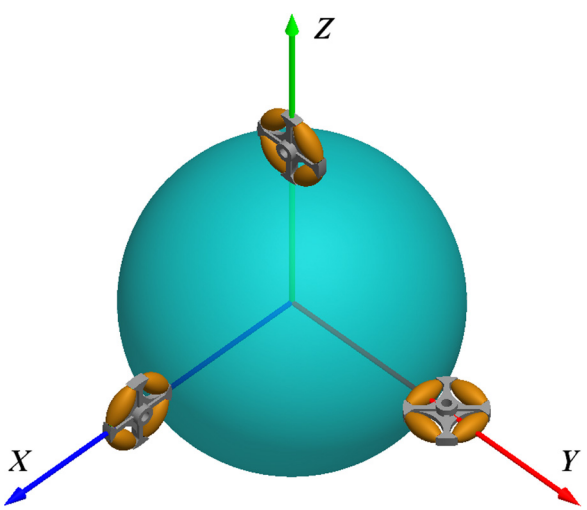

Fig. 7 Kinematic architecture for the orthogonal case

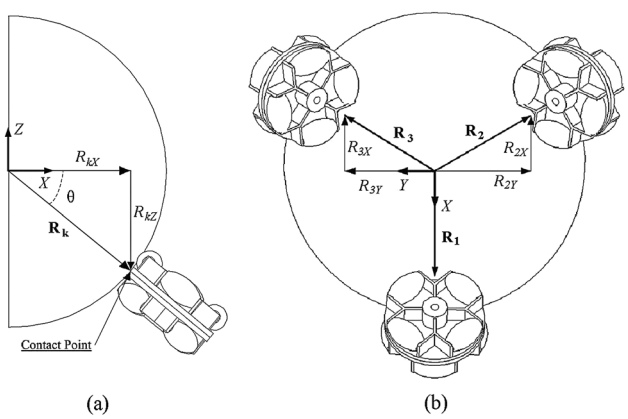

Fig. 8 Kinematic architecture for the Atlas sphere case

In this case

$$\begin{aligned}\vec{\mathbf{R}}_1 &= R(\cos\theta\hat{\mathbf{i}} - \sin\theta\hat{\mathbf{k}})\\ \vec{\mathbf{R}}_2 &= R\left(-\frac{1}{2}\cos\theta\hat{\mathbf{i}} - \frac{\sqrt{3}}{2}\cos\theta\hat{\mathbf{j}} - \sin\theta\hat{\mathbf{k}}\right)\\ \vec{\mathbf{R}}_3 &= R\left(-\frac{1}{2}\cos\theta\hat{\mathbf{i}} + \frac{\sqrt{3}}{2}\cos\theta\hat{\mathbf{j}} - \sin\theta\hat{\mathbf{k}}\right)\end{aligned} \tag{50}$$

and the contact point velocities are

$$\begin{aligned}\vec{\mathbf{V}}_1 &= -\omega_1 r\hat{\mathbf{j}}\\ \vec{\mathbf{V}}_2 &= \omega_2 r\left(-\frac{\sqrt{3}}{2}\hat{\mathbf{i}} + \frac{1}{2}\hat{\mathbf{j}}\right)\\ \vec{\mathbf{V}}_3 &= \omega_3 r\left(\frac{\sqrt{3}}{2}\hat{\mathbf{i}} + \frac{1}{2}\hat{\mathbf{j}}\right)\end{aligned} \tag{51}$$

as shown in Ref. [28]. These yield

$$\begin{bmatrix}\hat{\Omega}_1^T\\ \hat{\Omega}_2^T\\ \hat{\Omega}_3^T\end{bmatrix} = \begin{bmatrix}-\sin\theta & 0 & -\cos\theta\\ \frac{1}{2}\sin\theta & \frac{\sqrt{3}}{2}\sin\theta & -\cos\theta\\ \frac{1}{2}\sin\theta & -\frac{\sqrt{3}}{2}\sin\theta & -\cos\theta\end{bmatrix} \tag{52}$$

The determinant of this matrix will yield zero for

$$\frac{3\sqrt{3}}{2}\sin^2\theta\cos\theta = 0 \tag{53}$$

and so, the only singularities would be for $\theta = 0$ deg and $\theta = \pm 90$ deg. For all other cases, the Jacobian can be evaluated. In this case

$$\begin{aligned}\mathbf{J} &= \frac{r}{R}\begin{bmatrix}-\sin\theta & 0 & -\cos\theta\\ \frac{1}{2}\sin\theta & \frac{\sqrt{3}}{2}\sin\theta & -\cos\theta\\ \frac{1}{2}\sin\theta & -\frac{\sqrt{3}}{2}\sin\theta & -\cos\theta\end{bmatrix}^{-1}\\ &= \frac{r}{3R}\begin{bmatrix}-2\csc\theta & \csc\theta & \csc\theta\\ 0 & \sqrt{3}\csc\theta & -\sqrt{3}\csc\theta\\ -\sec\theta & -\sec\theta & -\sec\theta\end{bmatrix}\end{aligned} \tag{54}$$

Thereby, showing the direct relationship between omnidirectional wheel speeds and sphere angular velocity without kinematic slip for the single-row case. It is obvious once again that this case does not simultaneously fulfill the requirement for $n = 6$.

4.3 The Collinear Case. An example that conforms to both conditions of the triple-race case can easily be constructed.

In the configuration shown in Fig. 9 we have

$$\hat{R}_1 = \hat{i};\ \ \hat{R}_2 = \frac{\sqrt{2}}{2}\hat{i} + \frac{\sqrt{2}}{2}\hat{j};\ \ \hat{R}_3 = \hat{j} \tag{55}$$

$$\hat{\Omega}_1 = \hat{j};\ \ \hat{\Omega}_2 = \hat{k};\ \ \hat{\Omega}_3 = \hat{i} \tag{56}$$

and it is clear that the three induced angular velocities are linearly independent, while all position unit vectors lay in the XY plane, thus being linearly dependent.

4.4 Orthogonal Case with Six Omnidirectional Wheels. This example examines a case where six omnidirectional wheels are employed. First, arbitrary values for the speeds of the omnidirectional wheels will be assigned and the slip factor will be evaluated; then the same scenario will be investigated using the master-slave concept.

Here, the position vectors of the six contact points, as shown in Fig. 10 are

$$\begin{aligned}\vec{\mathbf{R}}_1 = R\hat{\mathbf{i}};\quad \vec{\mathbf{R}}_2 = R\hat{\mathbf{j}};\quad \vec{\mathbf{R}}_3 = R\hat{\mathbf{k}}\\ \vec{\mathbf{R}}_4 = -R\hat{\mathbf{i}};\quad \vec{\mathbf{R}}_5 = -R\hat{\mathbf{j}};\quad \vec{\mathbf{R}}_6 = -R\hat{\mathbf{k}}\end{aligned} \tag{57}$$

and the position vectors of the contact points with respect to the omnidirectional wheel centres of rotation are

$$\begin{aligned}\vec{\mathbf{r}}_1 = -r\hat{\mathbf{i}};\quad \vec{\mathbf{r}}_2 = -r\hat{\mathbf{j}};\quad \vec{\mathbf{r}}_3 = -r\hat{\mathbf{k}}\\ \vec{\mathbf{r}}_4 = r\hat{\mathbf{i}};\quad \vec{\mathbf{r}}_5 = r\hat{\mathbf{j}};\quad \vec{\mathbf{r}}_6 = r\hat{\mathbf{k}}\end{aligned} \tag{58}$$

The angular velocities of the omnidirectional wheels are

$$\begin{aligned}\vec{\omega}_1 = \omega_1\hat{\mathbf{j}};\ \ \vec{\omega}_2 = \omega_2\hat{\mathbf{k}};\ \ \vec{\omega}_3 = \omega_3\hat{\mathbf{i}}\\ \vec{\omega}_4 = \omega_4\hat{\mathbf{j}};\ \ \vec{\omega}_5 = \omega_5\hat{\mathbf{k}};\ \ \vec{\omega}_6 = \omega_6\hat{\mathbf{i}}\end{aligned} \tag{59}$$

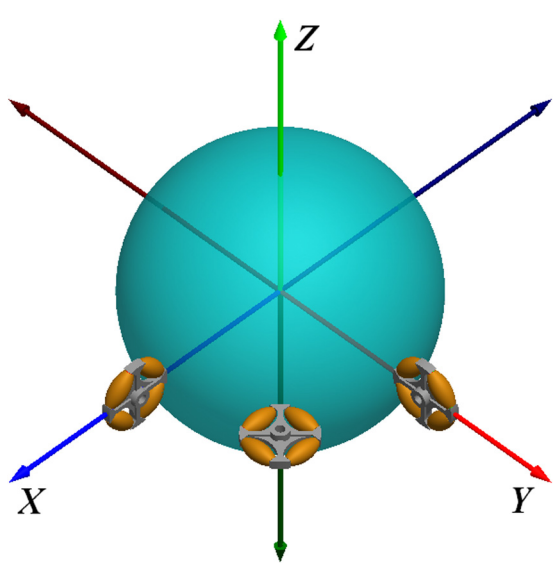

Fig. 9 A configuration that allows for slip-free conditions

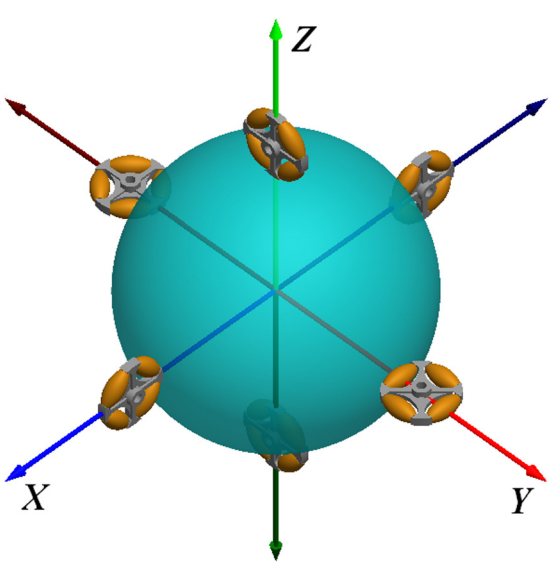

Fig. 10 Kinematic architecture for the orthogonal case with six omnidirectional wheels

and therefore the velocities they induce on the sphere at the contact points are

$$\begin{aligned}
\vec{\mathbf{V}}_1 &= \vec{\omega}_1 \times \vec{\mathbf{r}}_1 = \omega_1 r\hat{\mathbf{k}} \\
\vec{\mathbf{V}}_2 &= \vec{\omega}_2 \times \vec{\mathbf{r}}_2 = \omega_2 r\hat{\mathbf{i}} \\
\vec{\mathbf{V}}_3 &= \vec{\omega}_3 \times \vec{\mathbf{r}}_3 = \omega_3 r\hat{\mathbf{j}} \\
\vec{\mathbf{V}}_4 &= \vec{\omega}_4 \times \vec{\mathbf{r}}_4 = -\omega_4 r\hat{\mathbf{k}} \\
\vec{\mathbf{V}}_5 &= \vec{\omega}_5 \times \vec{\mathbf{r}}_5 = -\omega_5 r\hat{\mathbf{i}} \\
\vec{\mathbf{V}}_6 &= \vec{\omega}_6 \times \vec{\mathbf{r}}_6 = -\omega_6 r\hat{\mathbf{j}}
\end{aligned} \tag{60}$$

These velocities create the six components of angular velocity of the sphere

$$\begin{aligned}
\hat{\Omega}_1 &= \hat{\mathbf{i}} \times \hat{\mathbf{k}} = -\hat{\mathbf{j}} \\
\hat{\Omega}_2 &= \hat{\mathbf{j}} \times \hat{\mathbf{i}} = -\hat{\mathbf{k}} \\
\hat{\Omega}_3 &= \hat{\mathbf{k}} \times \hat{\mathbf{j}} = -\hat{\mathbf{i}} \\
\hat{\Omega}_4 &= -\hat{\mathbf{i}} \times -\hat{\mathbf{k}} = -\hat{\mathbf{j}} \\
\hat{\Omega}_5 &= -\hat{\mathbf{j}} \times -\hat{\mathbf{i}} = -\hat{\mathbf{k}} \\
\hat{\Omega}_6 &= -\hat{\mathbf{k}} \times -\hat{\mathbf{j}} = -\hat{\mathbf{i}}
\end{aligned} \tag{61}$$

Thus, we have

$$\left[\Omega^T\right] = \begin{bmatrix} 0 & -1 & 0 \\ 0 & 0 & -1 \\ -1 & 0 & 0 \\ 0 & -1 & 0 \\ 0 & 0 & -1 \\ -1 & 0 & 0 \end{bmatrix} \tag{62}$$

and the Jacobian becomes

$$\mathbf{J_{ls}} = \frac{r}{R}\begin{bmatrix} 0 & 0 & -0.5 & 0 & 0 & -0.5 \\ -0.5 & 0 & 0 & -0.5 & 0 & 0 \\ 0 & -0.5 & 0 & 0 & -0.5 & 0 \end{bmatrix} \tag{63}$$

This leads to the slip factor for the ith wheel being

$$S_i = \frac{1}{2}\left(1 - \frac{\omega_{((i+2)\bmod 6)+1}}{\omega_i}\right) \quad i = 1, 2, \ldots, 6 \tag{64}$$

Thus, the only way to obtain zero slip at all points requires

$$\omega_{((i+2)\bmod 6)+1} = \omega_i \quad \forall i \tag{65}$$

In other words, to enslave omnidirectional wheels 4, 5, and 6 to omnidirectional wheels 1, 2, and 3 or vice versa. Any other angular velocity combination would yield nonzero slip. For example, consider

$$\omega_1 = \omega_2 = \omega_3 = 1, \quad \omega_4 = \omega_5 = \omega_6 = 1.5 \tag{66}$$

resulting in a slip factor of $S = 0.52$.

5 Conclusions

The kinematics of a sphere actuated using omnidirectional wheels has been explored in a general way for the first time. The number of actuating wheels, as well as their type has been considered, and some specific configurations have been explored. The feasibility of the case $n = 3$ from the kinematics standpoint has been explored for a few configurations. A major conclusion is that a necessary condition for eliminating kinematic slip is that the three induced angular velocities $\vec{\Omega}_i$ must be linearly independent. This means that the singularities and slip issues that result from kinematic sources may be eliminated at the design stage, rather than relying on real-time control solutions. In addition, a Jacobian for the architecture was presented in its most general form, such that it applies to any configuration meeting the no-slip criteria presented for $n = 3$. The simplicity of the expressions obtained for the kinematics of the platform will also be advantageous when it comes to real-time computations. It should be noted that the Jacobian and slip analysis presented here differ from those presented in Refs. [28 and 29], and serve to correct them.

In addition, the case where $n > 3$ has been explored, with special attention given to the practical application to three-race omnidirectional wheels. Although designs that meet the no-slip conditions exist, as presented above, clearly, none of them could be singularity-free, while maintaining the no-slip conditions. Any three-race omnidirectional wheel solution would be kinematically-inferior to single-race and double-race [22] solutions, that were shown to have Jacobians that represent one-to-one mappings from the input angular speeds of the omnidirectional wheels to the output angular velocity of the sphere. It seems that while intuition suggests that the triple-race omnidirectional wheels may give the best of both worlds, the analysis suggests otherwise, since while for the single and dual-race cases zero slip is obtained throughout the entire workspace, triple-race wheels obtain them for only a fraction of the workspace, showing higher slip ratios for the remainder of the workspace, as demonstrated earlier. This deception of intuition may be explained by exploring the single degree-of-freedom case, where a single omnidirectional wheel would drive a sphere or a cylinder. In this simple case, the desired effect is accomplished; however, once more degrees of freedom are introduced, kinematic slip is imminent. However, the $n > 3$ case may still resolve the roller contact discontinuity issue inherent to omnidirectional wheels by employing a master-slave strategy, where the kinematics of the system depend upon three master omnidirectional wheels while the remaining omnidirectional wheels accept angular velocity values that are dictated by the master wheels to eliminate slip. A specific important case was demonstrated where equivalent antipodal contact points were employed for maintaining a constant offset between two equivalent antipodal omnidirectional wheels such that an equivalent antipodal continuous contact point yields a single constant Jacobian for the system.

The above findings do not eliminate the need to evaluate and minimize kinetically-induced slip, i.e., slip that results from contact forces and moments. However, the formulation presented here reveals conditions that lead to several classes of configuration, as demonstrated with two examples. From these results, optimal solutions can be selected based on practical criteria. For example, the requirement to eliminate kinetically-induced slip, minimize reaction forces, or minimize actuation power requirements could serve as design criteria.

Acknowledgment

The authors gratefully acknowledge the contribution to this work made by Andrew Dobson in creating the images in Figs. 1, 7, 9, and 10.

Nomenclature

J = Jacobian matrix
n = number of omnidirectional wheels
q = unit quaternion describing the orientation of the sphere
$\vec{R}_i$ = position vector of contact point i
$\hat{R}_i$ = unit vector in the direction of contact point i
R = radius of the sphere
r_i = radius of omnidirectional wheel i
S = slip assessment indicator
S_i = slip ratio at contact point i
$\vec{V}_i$ = velocity induced by omnidirectional wheel i
$\vec{V}'_i$ = velocity of the sphere at contact point i

$\hat{v}_i$ = unit vector in the actuation direction at contact point i
$\hat{v}_{r_i}$ = unit vector in the free-roll direction at contact point i
$\vec{\Omega}$ = angular velocity vector of the sphere
$\hat{\Omega}_i$ = unit induced angular velocity by omnidirectional wheel i
ω_i = angular speed of omnidirectional wheel i

References

[1] Gough, V. E., 1956-1957, "Contribution to Discussion of Papers on Research in Automobile Stability, Control and Tyre Performance," Proc. Auto. Div. Inst. Mech. Eng, **171**, pp. 392–394.
[2] Stewart, D., 1965, "A Platform With 6 Degrees of Freedom," Proc Inst. Mech. Eng., Part 1, **15**, pp. 371–386.
[3] Gosselin, C., 1990, "Determination of the Workspace of 6-DOF Parallel Manipulators," Journal of Mechanisms, Transmission, and Automation in Design, **112**(3), pp. 331–336.
[4] Yan, J., I-Ming, C., and Guilin, Y., 1990, "Kinematic Design of a 6-DOF Parallel Manipulator With Decoupled Translation and Rotation," IEEE Trans. Robot., **22**(3), pp. 545–551.
[5] Kim, J., Hwang, J. C., Jim, J. S., Iurascu, C. C., Park, F. C., Cho, Y. M., 2002, "Eclipse II: A New Parallel Mechanism Enabling Continuous 360-Degree Spinning Plus Three-Axis Translational Motions," IEEE Trans. Rob. Autom., **18**(3), pp. 367–373.
[6] Advani, S. K., 1998, "The Kinematic Design of Flight Simulator Motion-Bases," Ph.D. thesis, Delft University Press, 1998.
[7] Stock, M., and Miller, K., 2003, "Optimal Kinematic Design of Spatial Parallel Manipulators: Application to Linear Delta Robot," Trans. ASME J. Mech. Des., **125** (2), pp. 292–301.
[8] Fattah, A., and Agrawal, S. K., 2005, "On the Design of Cable-Suspended Planar Parallel Robots," Trans ASME J. Mech. Des., **127**(5), pp. 1021–1028.
[9] Merlet, J. P., 2006, "Jacobian, Manipulability, Condition Number, and Accuracy of Parallel Robots," Trans. ASME J. Mech. Des., **128**(1), pp. 199–206.
[10] Merlet, J. P., 2000, *Parallel Robots*, Kluwer Ac. Pub., Boston, MA.
[11] Hayes, M. J. D., and Langlois, R. G., 2005, "A Novel Kinematic Architecture for Six DOF Motion Platforms," Trans. Can. Soc. Mech. Eng., **29**(4), pp. 701–709.
[12] Lauwers, T. B., Kantor, G. A., and Hollis, R. L., 2005, "One is Enough!," *Proceedings of 2005 International Symposium of Robotics Research*.
[13] Ferriere, L., and Raucent, B., 1998, "ROLLMOBS, A New Universal Wheel Concept," *Proceedings of the 1998 IEEE International Conference on Robotics and Automation*, pp. 1877–1882.
[14] West, M., and Asada, H., 1995, "Design and Control of Ball Wheel Omnidirectional Vehicles," *Proceedings of IEEE International Conference on Robotics And Automation*, pp. 1931–1938.
[15] Williams, R., Carter, D., Gallina, P., and Rosati, G., 2002, "Dynamics Model With Slip for Wheeled Omni-Directional Robots," IEEE Trans. Rob. Autom., **18**(3), pp. 285–293.
[16] Saha, K., Angeles, J., and Darcovich, J., 1995, "The Design of Kinematically Isotropic Rolling Robots with Omnidirectional Wheels," Mech. Mach. Theory, **30**(8), pp. 1127–1137.
[17] Alexaner, J. C., and Maddocks, J. H., 1989, "On the Kinematics of Wheeled Mobile Robots," Int. J. Robot. Res., **8**(5), pp. 15–27.
[18] Low, K. H., and Leow, Y. P., 2005, "Kinematic Modeling, Mobility Analysis and Design of Wheeled Mobile Robots," Adv. Rob., **19**, pp. 73–99.
[19] Yu, H., Dubowsky, S., and Skwersky, A., 2000, "Omni-Directional Mobility Using Active Split Offset Castors," *Proceedings of the 26th Biennial Mechanisms and Robotics Conference of the 2000 ASME Design Engineering Technical Conferences*.
[20] Hayes, M. J. D., Langlois, R. G., and Weiss, A., 2008, "Atlas Motion Platform Generalized Kinematic Model," *Proceedings of the Second International Workshop on Fundamental Issues and Future Research Directions for Parallel Mechanisms and Manipulators*, September 21-22, Montpellier, France.
[21] Hayes, M. J. D., Langlois, R. G., and Weiss, A., 2011, "Atlas Motion Platform Generalized Kinematic Model," Meccanica, **46**(1), pp. 17–25.
[22] Weiss, A., Langlois, R. G., and Hayes, M. J. D., 2009, "The Effects of Dual-Row Omnidirectional Wheels on the Kinematics of the Atlas Spherical Motion Platform," J. Mech. Mach. Theory, **44**(2), pp. 349–358.
[23] Weiss, A., Langlois, R. G., and Hayes, M. J. D., 2008, "Kinematics of the Atlas Platform with Redundant Contact Points," *CSME Symposium on Machines, Mechanisms and Mechatronics*, on CD, Ottawa, Canada, June 2008.
[24] Leow, Y. P., Low, K. H., and Loh, W. K, 2002, "Kinematic Modelling and Analysis of Mobile Robots With Omni-Directional Wheels," *Proceedings of the 7th International Conference on Control, Automation, Robotics and Vision, ICARCV 2002*, pp. 820–825.
[25] Angeles, J., 2003, *Fundamentals of Robotic Mechanical Systems: Theory, Methods, and Algorithms*, 2nd ed., Springer-Verlag, New York.
[26] Angeles, J., 1988, *Rational Kinematics*, Springer-Verlag, New York.
[27] Schwab, A. L., and Meijaard, J. P., 2006, "How to Draw Euler Angles and Utilize Euler Parameters," *Proceedings of ASME IDETC/CIE 2006*, September 10-13.
[28] Holland, J. B., Hayes, M. J. D., and Langlois, R. G., 2005, "A Slip Model for the Spherical Actuation of the Atlas Motion Platform," Trans. Can. Soc. Mech. Eng, **29**(4), pp. 711–720.
[29] Robinson, J., Holland, J. B., Hayes, M. J. D., and Langlois, R. G., 2005, "Velocity-level Kinematics of a Spherical Orienting Device Using Omni-directional Wheels," Trans. Can. Soc. Mech. Eng., **29**(4), pp. 691–700.